Int. J. Electrochem. Sci., 12 **(2017)** 4488 – 4501, doi: 10.20964/2017.05.08

International Journal of ELECTROCHEMICAL SCIENCE
www.electrochemsci.org

Low Potential Determination of NADH at 1-Hydroxypyrene/reduced Graphene Oxide Modified Electrode

Xiujuan Wu, Miaomiao Yu, Xiaowang Liu, Maoguo Li[*]

Anhui Key Laboratory of Chemo-Biosensing, College of Chemistry and Materials Science, Anhui Normal University, Wuhu 241000, China
[*]E-mail: limaoguo@mail.ahnu.edu.cn

Received: 8 February 2017 / *Accepted:* 5 March 2017 / *Published:* 12 April 2017

This work presents a facile method to availably synthesize the reduced graphene oxide (rGO), which utilizes the dopamine (DA) as the reducing agent. PDA/rGO was prepared by the simultaneous reduction of GO with dopamine hydrochloride and the self-polymerization of dopamine. The surface polydopamine (PDA) film was removed by immersing in a strong alkali solution (pH>10) to obtain the pure rGO. Then 1-hydroxypyrene (1-OHP) was absorbed on the surface of rGO modified glassy carbon electrode (GCE) via π-π stacking interaction to fabricate a 1-OHP-rGo modified GCE (denoted as 1-OHP/rGO/GCE). The synergistic effect between the 1-OHP and rGO effectively reduced the oxidation over-potential of nicotinamide adenine dinucleotide (NADH), which realized the determination of NADH under relatively low potential (-0.06 V *vs.* SCE), which negatively shift 623 mV compared with that at the bare GCE. Further, the amperometric response of the modified electrode to NADH shows a linear concentration range of 100 μM to 3800 μM with the calculated limit of detection of 14.8 μM at a signal-to-noise ratio of 3. We expect that this biosensor could be used for determination of NADH in biosamples.

Keywords: nicotinamide adenine dinucleotide; graphene; biosensors; polydopamine; 1-hydroxypyrene

1. INTRODUCTION

NAD^+/NADH (nicotinamide adenine dinucleotide) is an indispensable co-enzyme couple found in the enzymatic reactions of over 300 dehydrogenases that has possible application in food processing, environmental analysis, and clinical diagnosis [1-6]. Beside these, NADH is also of great medicinal significance as it improves the functioning of people suffering from diseases like Alzheimer, Parkinson's disease and depression etc [7-9]. Thus, it is of considerable interest to prepare sensors for monitoring NADH levels in biological systems.

However, the direct electro-oxidation of NADH at conventional bare electrode surfaces is highly irreversible and requires a large over-potential due to its high activation energy [10-13]. Therefore, many unwanted side reactions from electro-active interferences can cause loss of selectivity, reproducibility and stability [14, 15]. Utilizing efficient electron-transfer mediators is an effective method to reduce the high over-potential and minimize the electrode fouling. Conventional and efficient mediators include quinones [16, 17], organic dye molecules [18, 19] and metal oxides [12, 20, 21].

In the recent decades, with the development of nanotechnology, nanomaterials-based especially carbon-based electrochemical biosensors have been of great interest due to their unique structural and electrical properties [20]. For example, Hanzi et al. used electrochemically activated carbon materials to facilitate high-rate NADH electro-catalysis for bioconversion, biosensor and bioenergy processes [19]. Jacob et al. investigated the electro-catalytic oxidation of NADH at nitrogen-doped carbon nanotube electrode, which implied the dehydrogenase enzyme kinetics through electrochemical measurement [14]. Marilyn et al. found the relationship between the state of the surface of carbon nanotubes (CNTs) and their electrochemical activity toward the NADH by different treatment of carbon nanotubes [22]. A novel electrochemical biosensing platform for NAD^+-dependent dehydrogenase was prepared using the nitrogen-doped graphene (NG) [23].

1-Hydroxypyrene (1-OHP), containing two aromatic rings, is easily oxidized to o-quinone through two steps of electrochemical oxidation. It is well known that quinones are efficient electron-transfer mediators toward NADH oxidation [17]. However, since its bad conductivity, we need to find a material with good conductivity to support it. Graphene is a brilliant candidate for adsorption of 1-OHP through π-π stacking effect due to its highly delocalized π electrons [24].

Graphene, a one-atom-thick planar sheet of sp^2-bonded carbon atoms with a honeycomb two-dimensional lattice [25], has attracted widespread attention in the fields of electrochemical sensor and biosensor owing to its unusual electronic conductivity, high specific surface area, high mechanical, thermal and chemical stabilities [26, 27]. Graphene not only can provide a biocompatible microenvironment for enzymes but also enhance direct electron transfer between the enzymes and substrate electrodes. With the above considerations, graphene is very attractive as support matrices for enzymes immobilization owing to their intrinsic properties and unique structures [28]. However, their application is limited by the aggregation of graphene. The chemically reduced graphene oxide (rGO) naturally has a tendency to agglomerate irreversibly, or even to restack into graphite through van der Waals interactions. Therefore, it is imperative to seek effective and mild methods for the reduction of graphene oxide (GO), as well as modification of graphene by introducing functional groups to improve its stability and dispersibility [29]. So far, there has been many synthesis method of graphene reported, such as chemical, thermal, electrochemical and so on. Among these methods, chemical reduction is most popular. Main reductants are hydrazine, dimethyl hydrazine and sodium borohydride, sulfoxide chloride, etc. However, these reductant are toxic and can cause a certain degree of damage on the the prepared graphene layers structure [25, 30, 31].

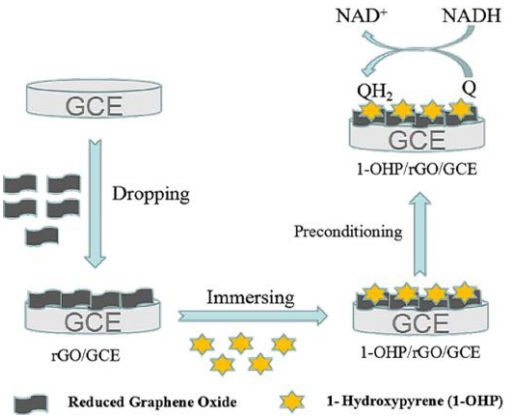

Scheme 1. Schematic representation of the electrochemical experiment process.

In this work, graphene oxide (GO) was mildly reduced by dopamine to prepare reduced graphene oxide (rGO) which was employed as a supporting material to load 1-OHP. Scheme 1 represents the electrochemical experiment process. The 1-OHP was transferred to o-quinone containing two aromatic rings to electro-catalytic oxidation of NADH by two steps of electrochemical oxidation. The overpotential of NADH oxidation was greatly decreased (623 mV).

2. EXPERIMENTAL

2.1. Regents and chemicals

Nafion (5 wt% solution in a mixture of lower water) was purchased from Aldrich and used as received. All chemicals were of analytical grade and used without further purification. The Graphene Oxide Solution was purchased from Chengdu Organic Chemicals Co. Ltd. 1-OHP solution was prepared from 50% methanol/water mixture. All the other solutions were prepared from ultrapure water (Millipore, 18.25 MΩ·cm, 25 ^{o}C). NADH (β-nicotinamide adenine dinucleotide, reduced form), Glucose, glutathione (reduced) were purchased from Sangon Biotech (Shanghai). The phosphate buffer solutions (PBS) with different pHs were prepared by mixing the stock solutions of Na_2HPO_4 and NaH_2PO_4, and adjusted the pH with 0.1 M NaOH or H_3PO_4 solution. The solutions were purged with highly purified nitrogen for at least 20 min before the experiments and nitrogen atmosphere was maintained over the solutions during the experiments.

2.2. Synthesis of reduced graphene oxide (rGO)

The reduced graphene oxide (rGO) was prepared using a chemical reduction method reported [32]. 2 mL 10 mg mL^{-1} graphene oxide (GO) was diluted by 30 mL water by sonication for 30 min. Then 10 mg of dopamine hydrochloride was added and the mixture was stirred for 60 min at room temperature. Subsequently 8 mL of 50 mM Tris-HCl solution (pH 8.5) was added, the reaction mixture

was stirred at 80 ^{o}C for 24 h. After cooled down to room temperature, 1 M NaOH was added to the solution to adjust the pH greater than 10 and stirred at room temperature overnight. Then the solution was centrifuged and washed until the pH was neutral. Finally the product was dried at 60 ^{o}C for 24 h.

2.3. Sensor construction

Prior to the electrode modification, the bare glassy carbon (GC) electrode surface was polished with 1, 0.3, 0.05 μm alumina slurry, respectively, and then cleaned by sonication to remove any adhesive. The cleaned GC electrode was dried with nitrogen steam for the next modification. Then 3 μL 1 mg mL^{-1} rGO suspension was dropped on the GC electrode surface and dried at room temperature. Subsequently the rGO/GC electrode was immersed in 5 μM 1-OHP solution for the interval of time. Finally the modified electrode was rinsed with ultrapure water and dried at room temperature. Thus, the 1-OHP/rGO/GC electrode was successfully prepared.

2.4. Apparatus and measurements

The size and morphology of the prepared rGO were recorded by a HT-7700 transmission electron microscope (TEM) operated at 120 kV. The energy dispersive X-ray spectroscopy (EDX) images were obtained by an S-4800 field-emission scanning electron microscope (SEM).

All electrochemical measurements were performed with CHI660C electrochemical workstation (CH Instruments, Shanghai, China). A conventional three-electrode system was employed with GC electrode or modified electrode as working electrode, saturated calomel electrode (SCE) as the reference electrode, platinum electrode as the counter electrode. Electrochemical impedance spectroscopy (EIS) was performed in the presence of a 5 mM $K_3Fe(CN)_6/K_4Fe(CN)_6$ and 0.1 M KCl by applying an AC voltage with 5 mV amplitude in a frequency range from 0.01 Hz to 10^5 Hz under open circuit potential conditions. When studying the electrochemical properties of 1-OHP, Cyclic voltammetry (CV) was performed in phosphate buffer solution (PBS) (50 mM, pH 2.0) containing NaCl (0.2 M) with a potential window from -0.6 V to 0.8 V. When studying the electrocatalytic oxidation of NADH, CV was performed in 0.1 M pH 7.0 PBS with a potential window from -0.45 V to 0.8 V. Differential pulse voltammetry (DPV) was performed in PBS (50 mM, pH 2.0) containing NaCl (0.2 M). Amperometric i-t Curve was performed in 0.1 M pH 7.0 PBS at applied potential of -0.06 V (*vs.* SCE). All electrochemical experiments were carried out in nitrogen-purged solutions at room temperature.

3. RESULTS AND DISCUSSION

3.1. Characterizations of rGO

The morphology of the prepared rGO was examined by TEM shown in Figure. 1A. The reduced graphene oxide nanosheet presented a thin structure with a number of tiny wrinkles over the whole surface owing to the thin structure of the sheet [33].

The energy dispersive X-ray spectroscopy (EDX) has been widely used as an effective method to measure the types and contents of elements. From Figures. 1C and 1D, we can distinctly observe the content of oxygen has greatly decreased after reaction, which demonstrated GO was reduced to rGO successfully. Moreover, we cannot find any nitrogen in the prepared rGO. It proved that the PDA film has been removed from the surface of rGO.

The measurement of conductivity can also demonstrate the rGO was successfully synthesized. Figure. 1B displayed the impedance spectrum of rGO compared with PDA, PDA-rGO, GO, and bare GCE. The electron-transfer resistance (R_{et}) of rGO was much lower than that of PDA, PDA-rGO and GO. which testified that dopamine triumphantly reduced the GO to rGO and the PDA film was also removed [29, 33].

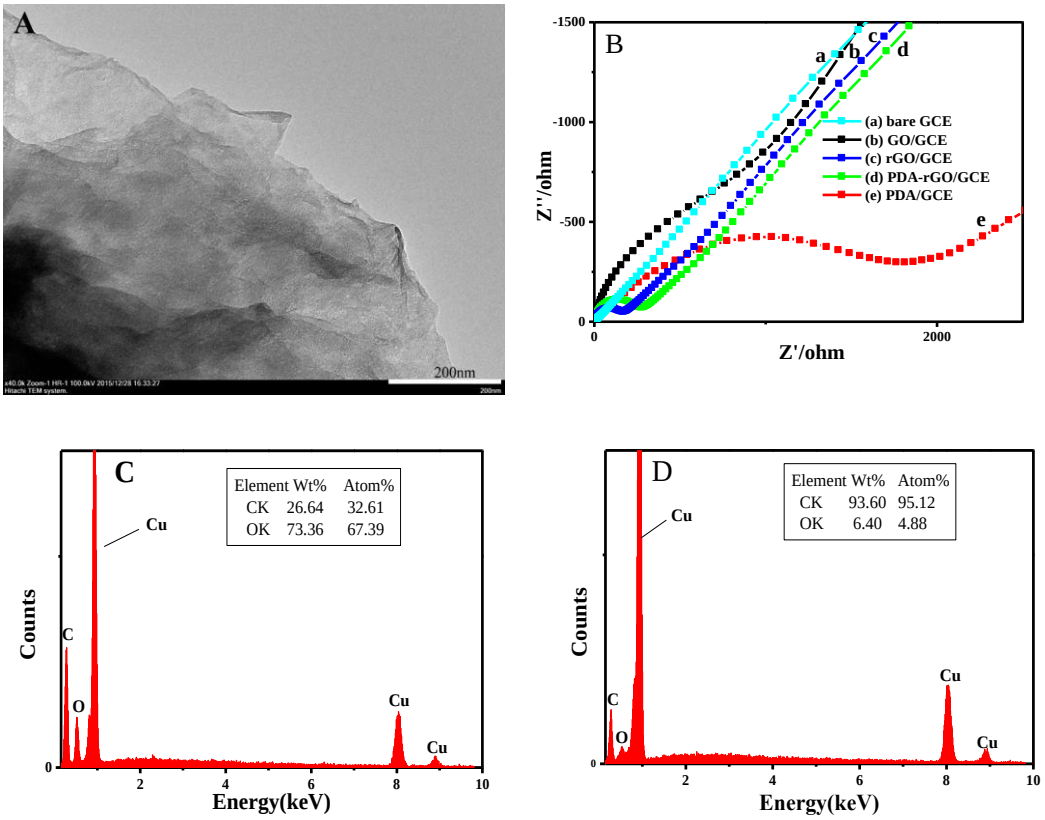

Figure 1. (A) The TEM image of rGO. The scale bar is 200 nm. (B) Nyquist plots of (a) bare GCE, (b) GO/GCE, (c) rGO/GCE, (d) PDA-rGO/GCE, (e) PDA/GCE in 5 mM $K_3Fe(CN)_6/K_4Fe(CN)_6$ containing 0.1 M KCl. EDX images of (C) GO, (D) rGO.

3.2. Electrochemical behavior of 1-OHP on the rGO modified electrode

Electrochemical characteristics of 1-OHP on the rGO modified electrode are displayed in Figure. 2A. When 1-OHP is absent, there are no redox peaks in the CVs. The high background current of rGO modified electrode is due to the large surface area and good conductivity of rGO. After pre-concentrated with 1-OHP, a pair of redox peaks around 0.2 V appear clearly, suggesting the 1-OHP was successfully absorbed. Additionally, there is a strong oxidation peak near 0.6 V in the first scan,

which is gradually reduced as scanning going on. This oxidation peak is attributed to first irreversible oxidation of 1-OHP. It was demonstrated that the reaction of 1-OHP on these electrodes consisted of two processes: one step of irreversible oxidation and one step of reversible oxidation. The proposed oxidation mechanism is shown in Figure. S1 [34]. The oxidation peak current of 1-OHP on the GO modified electrode (Figure. 2B, curve b) is only slightly greater that on the bare electrode (Figure. 2B, curve a) demonstrating the weak interaction between GO and 1-OHP. Also, the oxidation peak currents of 1-OHP on the PDA-rGO (Figure. 2B, curve c) and rGO modified electrodes (Figure. 2B, curve d) are much more higher than as compared with GO modified electrode. The above results indicate that the starting GO was reduced by dopamine, which leads to the increase of conductivity. However, the oxidation peak currents of 1-OHP on the PDA-rGO is lower than that of rGO modified electrode, which is ascribed to the surface film of polydopamine that can hinder the interaction between rGO and 1-OHP.

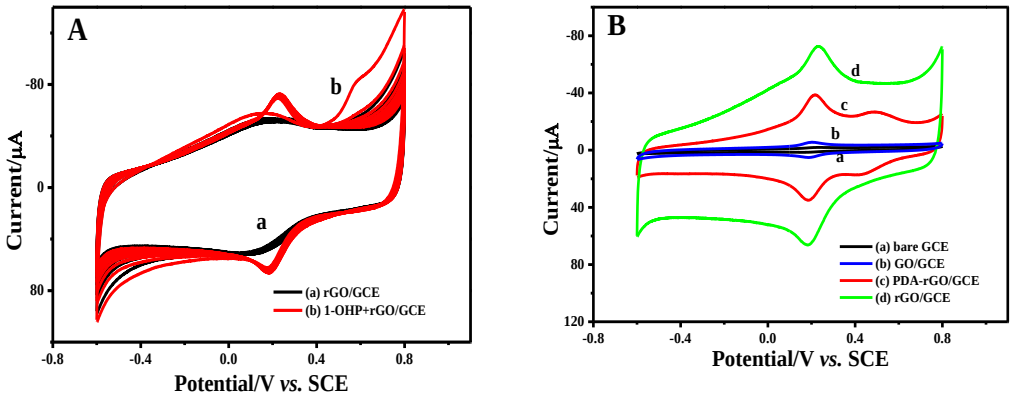

Figure 2. (A) Successive 10 cycles' scan of (a) rGO/GCE, (b) 1-OHP at rGO/GCE. (B) CVs of 1-OHP at (a) bare GCE, (b) GO/GCE, (c) PDA-rGO/GCE, (d) rGO/GCE in 0.05 M pH 2.0 PBS containing 0.2 M NaCl after 10 cycles' scan. The scan rate is 100 mV s^{-1}.

In order to investigate the surface dynamical process of 1-OHP/rGO/GCE, we explored the effect of scan rate on the redox peak currents of the 1-OHP absorbed in rGO, which is shown in Figure. 3A. Cathodic and anodic peak potentials perform a small shift and the peak currents increased as the scan rate from 5 to 400 mV/s. Simultaneously, Figure. 3B shows that the cathodic and anodic peak currents were linearly proportional to the scan rate in the whole range (linear relationship R=0.99966), which supporting the idea of a surface-confined redox process. The surface coverage which estimated the surface concentration of 1-OHP was obtained by using the Faraday's law, Γ = Q/nFA. In this case, Q is the charge from the area under the anodic peak of 1-OHP, A is the electro-active surface area of the electrode (0.07 cm^2). The surface coverage was calculated as 5.348×10^{-10} mol cm^{-2} for n = 2 on the rGO modified electrode. This value is five times larger than that of on the GO modified electrode (1.142×10^{-10} mol cm^{-2}) and 17.7 times larger than the bare glassy electrode (3.023×10^{-11} mol cm^{-2}) [35]. These results presented in Table S1 prove that effective π-electron system of rGO plays a great role in the high amount of 1-OHP loading on rGO. Changes in solution pH have

been shown to greatly impact the formal potential of the redox couples of 1-OHP, which exhibits much better electrochemical activities in acidic solution than in alkali solution. As shown in Figure. 3C, the peak currents gradually increased and the peak potentials shifted toward the negative direction. What is more, Figure. 3D reveals that the anodic peak potentials depended linearly on the pH according to the following equations: E_{pa}= -0.05488pH + 0.34611, with a slope of -54.88 mV pH^{-1}. The slope is close to the theoretical value of 59.0 mV pH^{-1} at 25 °C for two-protons-transfer coupled with two-electrons-transfer reaction [23], which was consistent with the mechanism demonstrated in Figure. S1.

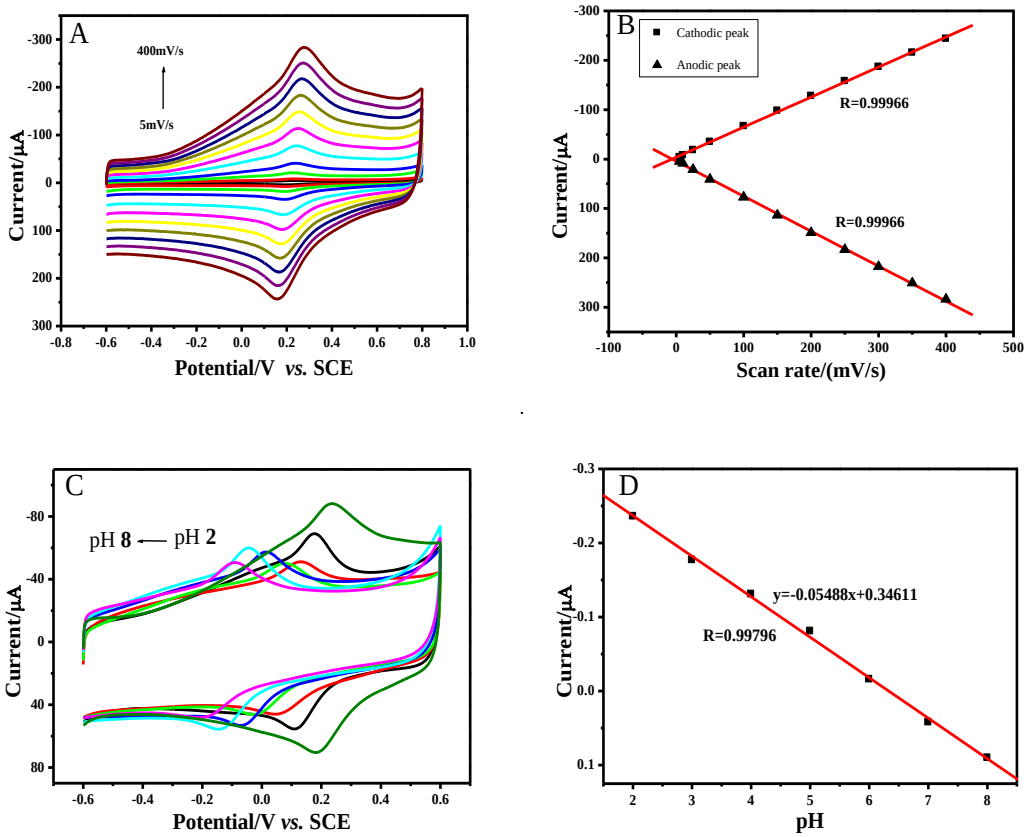

Figure 3. (A) CVs of 1-OHP on the rGO modified electrode with different scan rates: 5, 10, 25, 50, 100, 150, 200, 250, 300, 350, 400 mV s^{-1} in PBS (50 mM, pH 2.0) containing NaCl (0.2 M). (B) Plots of cathodic and anodic peak currents against scan rate. (C) CVs of 1-OHP on the rGO modified electrode in PBS (50 mM) containing NaCl (0.2 M) with different pH values of 2, 3, 4, 5, 6, 7, 8. The scan rate is 100 mV s^{-1}. (D) Plots of the anodic peak potentials against pH.

Electrochemical impedance spectroscopy (EIS) is an effective method for examining the electrical interfacial properties of surface-confined electro-active species (Figure. 4). For bare electrode, a small partially resolved semicircle in high frequency range attributed to the charge transfer resistance with a value of 100 Ω, while rGO/GCE exhibited almost a straight line in both high frequency range and low frequency range, suggesting the rGO possesses the ability of rapid electron transfer. After immersed in 1-OHP, the charge transfer resistance of 1-OHP/rGO/GCE was remarkably

enhanced by introducing the oxygen-related groups. Therefore, we can speculate that 1-OHP was successfully functioned on the rGO electrode.

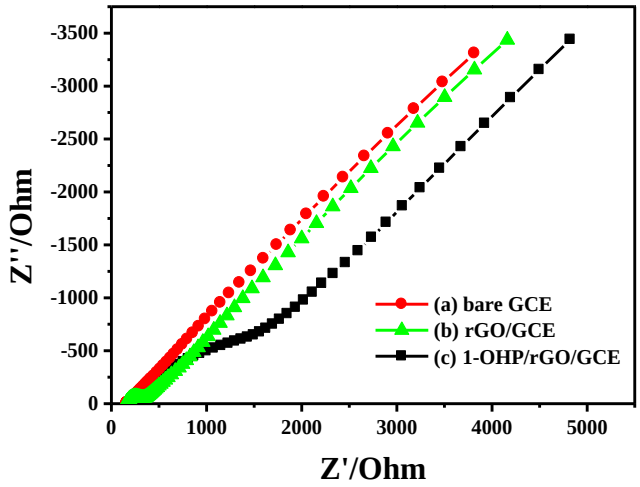

Figure 4. Nyquist plots of (a) bare GCE, (b) rGO/GCE, (c) 1-OHP/rGO/GCE in 2.5 mM $K_3Fe(CN)_6/K_4Fe(CN)_6$ containing 0.1 M KCl.

Differential pulse voltammetry (DPV) was employed to explore the effect of soaking time on the amount of 1-OHP absorbed on the electrode due to its high sensitivity and resolution than CV. After pre-concentrated with 1-OHP for 20, 40, 50, 60, 70, 80, 90 min, the DPV peak currents increased gradually and tended to be stable after 70 min. Apparently, the 70 min was selected as the optimal absorption time. After pre-concentrated with 1-OHP for 70 min, the DPV peak current of 1-OHP/rGO/GCE was greatly higher than that of 1-OHP/GCE, which is presented in Figure. S2. The results are owing to the strong π-π interaction between rGO and 1-OHP.

3.3. Electro-catalytic oxidation of NADH at 1-OHP/rGO modified GC electrode after electrochemical treatment

From the oxidation mechanism shown in Figure. S1, we can see that redox active quinones which can mediate electron transfer from NADH were formed during the oxidation process of 1-OHP. Therefore, we utilized the quinones to fabricate a modified electrode capable of the electro-catalytic oxidation of NADH. The electro-catalytic activity of the modified electrode was studied via concentration study. As shown in Figure. 5, curve b and a are CVs of the 1-OHP/rGO modified GC electrode after being anodizing at 0.8 V for 1000 s in PBS (pH 7.0) with and without NADH, respectively. When NADH is absent, there is no electro-catalytic oxidation peak. However, in the presence of NADH, a remarkable catalytic oxidation current at the modified electrode occurs at ca. -0.062 V, which negatively shift 623 mV, compared with that at the bare GCE (ca. 0.561 V). Furthermore, the electro-catalytic current increases significantly with a further increase of the concentration of NADH (Figure. S3). We can also find an oxidation peak near 0.4 V when the concentration of NADH is more than 1.5 mM, which is owing to the direct electrochemical oxidation

of NADH on 1-OHP/rGO/GCE that cannot be detected under such a low sensitivity. Thus, the shift in the peak potential can be attributed to the redox mediation of NADH oxidation by surface quinones generating in the oxidation process of 1-OHP. The electro-catalytic oxidation mechanism of NADH is displayed as follows:

Firstly, the surface quinones react with NADH through a chemical redox reaction: $Q+NADH \rightarrow QH_2+NAD^+$ (1), then the regeneration of quinone species is proceeded through the following electrochemical reaction: $QH_2 \rightarrow Q+2e^-+2H^+$ (2) [22]. The electrochemical results demonstrate that the electrochemical-treated 1-OHP/rGO modified GC electrode exhibits a good electrochemical catalytical activity of NADH and can be applied to the field of electrochemistry.

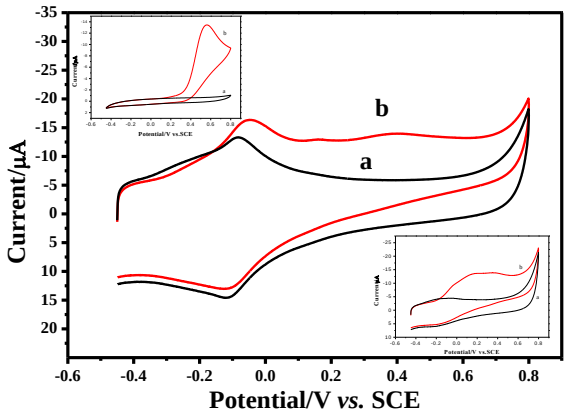

Figure 5. CVs of 1-OHP/rGO modified GC electrode with anodic polarization at 0.8 V for 1000 s in (a) 0.1 M pH 7.0 PBS, (b) 0.1 M pH 7.0 PBS containing 2.0 mM NADH. Inset are CVs of bare (upper) and untreated rGO modified (lower) electrodes in (a) 0.1 M pH 7.0 PBS, (b) 0.1 M pH 7.0 PBS containing 2.0 mM NADH. The scan rate is 20 mV s^{-1}.

3.4. Amperometric sensing of NADH

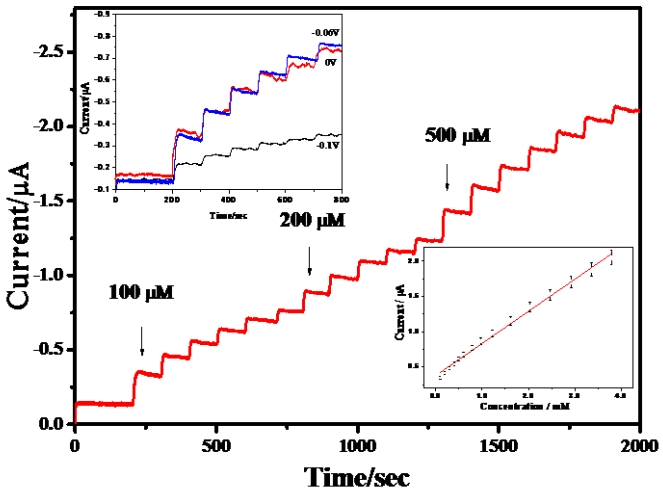

Figure 6. Amperometric response of 1-OHP/rGO/GC electrode for the oxidation of NADH at -0.06 V in 0.1 M PBS (pH 7.0). Inset: the upper is the optimization of applied potential, the lower is the calibration curve of I-C by i-t curve.

Figure. 6 displays the amperometric response of 1-OHP/rGO/GC electrode for the oxidation of NADH at -0.06 V in 0.1 M PBS (pH 7.0). The steady-state current response was achieved within 3 seconds following each addition of NADH, revealing a fast electron transfer between electrode surface and NADH. The calibration curve presents two linear concentration ranges: one from 0.1 mM to 1.5 mM, the other from 1.5 mM to 3.8 mM. The limit of detection was calculated to be 14.8 μM by $3\sigma/s$, where σ is the standard deviation of the blank PBS solution and s is the slope of the calibration curve.

Table 1. Comparison of the analytical property of different electrode materials for the detection of NADH. All the potentials refer to an Ag/AgCl electrode.

Electrode material	Potential (V)	Linear range (μM)	LOD (μM)	Reference
Au nanoparticle/rGO/GCE	0.55	0.050-500	0.0011	[8]
Co_3O_4 nanosheet/carbon ink	0.1	10-100	4.23	[10]
DNA/graphene/MB[a]/GCE	0.1	100-1500	1.0	[18]
Fe_3O_4/MWCNTs[b]/GCE	0	1-70,70-300	0.3	[20]
rGO/GC electrode	0.32	10-600	0.33	[35]
1-OHP/rGO/GCE	-0.01	100-3800	14.8	This work

[a] Multiwall carbon nanotubes

[b] Methylene blue

The comparison of analytical property of different electrode materials for the detection of NADH are listed in Table 1. The main advantage of our electrode is the large decrease in the over-potential of NADH oxidation. The results indicate that the 1-OHP/rGO/GC electrode is much more selective and stable, although the detection limit is a little high.

3.5. Selectivity, stability and reproducibility of the sensor.

Figure. 7 presents the interference study of several electro-active species. After separately added 2 mM interferent, the DPV response of 1-OHP/rGO/GC electrode displayed no obvious change. The 1-OHP/rGO /GC electrode also demonstrates an excellent stability of amperometric NADH response. Figure. S4 shows the amperometric response of 1-OHP/rGO modified GC electrode to 1 mM NADH over a continuous period of 2000 s. The current maintained nearly 90% after 2000 s. Five 1-OHP/rGO/GC electrodes were measured independently for the DPV response of 1 mM NADH. We found the RSD value of the different modified electrodes is 2.5%, and the RSD value of the different measurement of a modified electrode is 1.8%. From the above data and Figure. S5, we can draw a conclusion that the reproducibility of 1-OHP/rGO/GC electrode is acceptable.

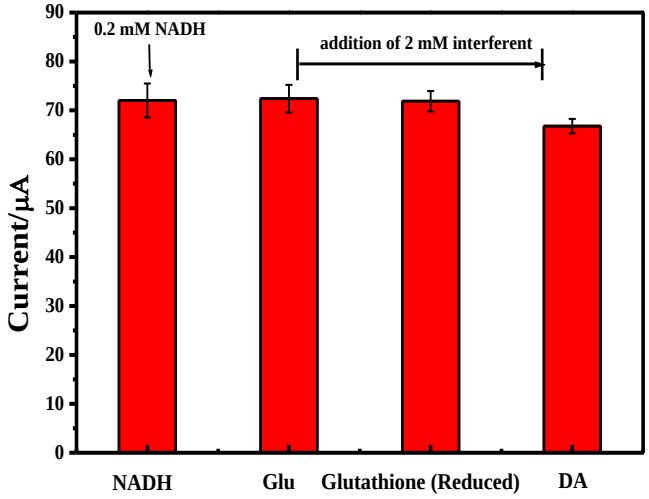

Figure 7. DPV response currents of 1-OHP/rGO/GCE in 0.1 M PBS (pH 7.0) containing 0.2 mM NADH or 0.2 mM NADH with 2 mM interferent. The concentration is the final state. All experiments were performed three times.

4. CONCLUSION

This work has successfully utilized a facile and eco-friendly reducing agent for the preparation of reduced graphene oxide. The removing of PDA film by immersing in strong alkali solution has greatly enhanced the conductivity of rGO. Then 1-OHP was absorbed on the surface of rGO modified electrode via π-π stacking interaction. The synergistic impact between the 1-OHP and rGO offered much improved and stable electro-catalytic activity toward the oxidation of NADH. The modified electrode has been shown to be promising for the development of NAD^+-dependent dehydrogenase electrochemical biosensors.

SUPPLEMENTARY MATERIAL

Low potential determination of NADH at 1-Hydroxypyrene/graphene modified electrode

Table S1. The surface coverage of different electrode material

Electrode material	1-OHP/ GCE	1-OHP/GO/GCE	1-OHP/rGO/GCE
Surface coverage	3.023×10^{-11} mol cm^{-2}	1.142×10^{-10} mol cm^{-2}	5.348×10^{-10} mol cm^{-2}

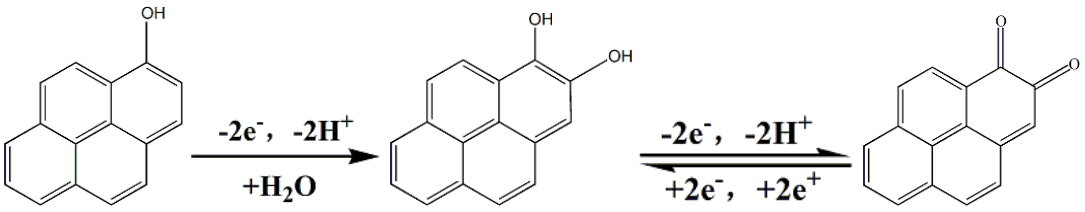

Fig. S1. Proposed oxidation mechanism of 1-OHP.

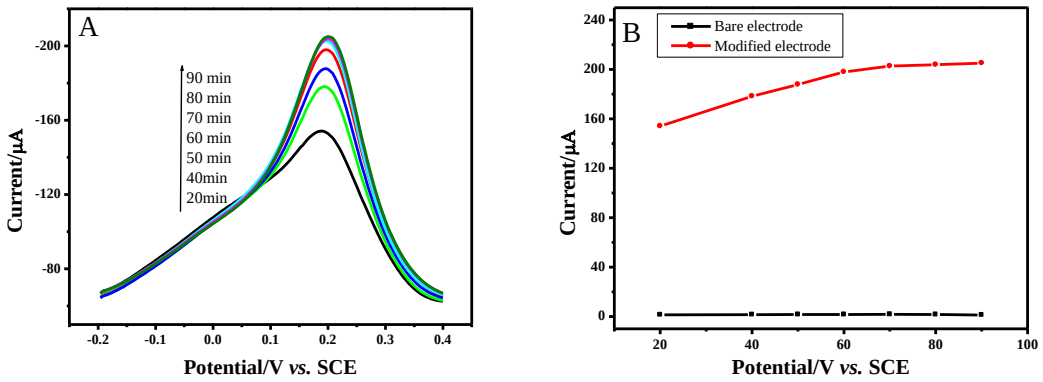

Fig. S2. (A) DPV curves of 1-OHP pre-concentrated on the rGO modified electrode for 20, 40, 50, 60, 70, 80, 90 min. (B) The relationships between the DPV peak currents and the pre-concentrated times of 1-OHP on rGO modified electrode and bare electrode.

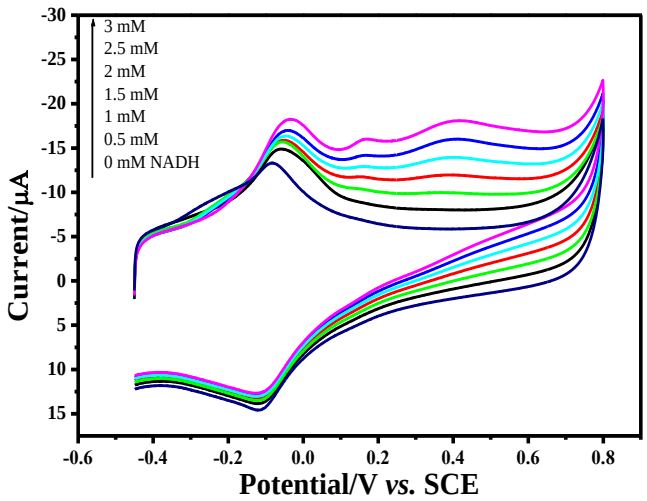

Fig. S3. CVs of 1-OHP/rGO modified GC electrode in 0.1 M pH 7.0 PBS containing (a-f) 0 mM, 0.5 mM, 1.0 mM, 1.5 mM, 2.0 mM, 2.5 mM, 3.0 mM NADH repectively. The scan rate is 20 mV s^{-1}.

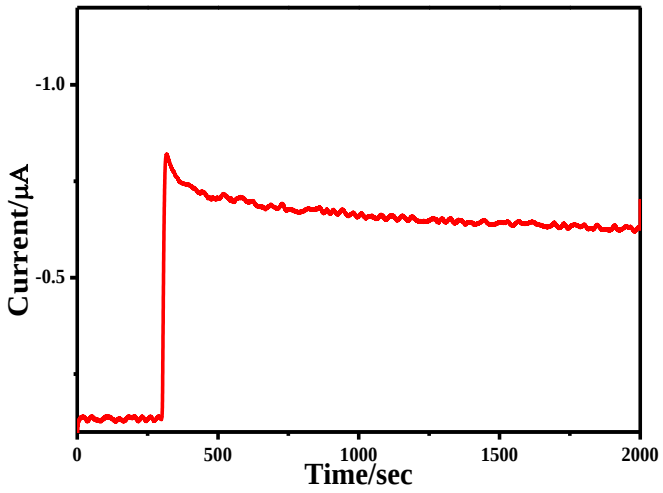

Fig. S4. Stability of current response of 1mM NADH at 1-OHP/rGO/GC electrode at applied potential of -0.06 V in 0.1 M PBS (pH 7.0).

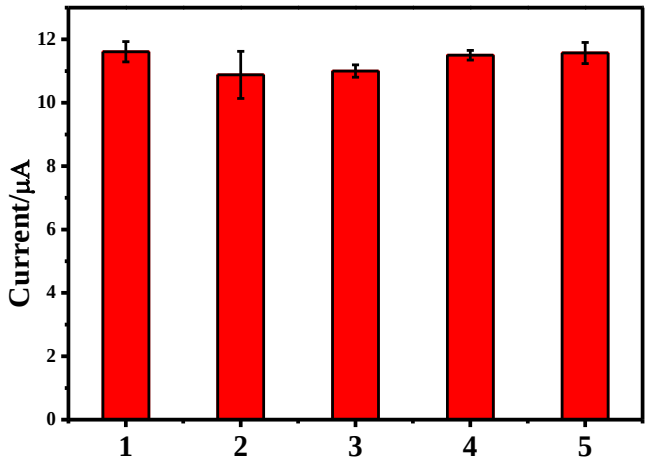

Fig. S5. DPV response currents of five 1-OHP/rGO/GCE in 0.1 M PBS (pH 7.0) containing 1 mM NADH. All experiments were performed three times.

ACKNOWLEDGEMENT
Dr. X.W. Liu is grateful for the financial support from the National Natural Science Foundation of China (21471007). This work is also supported by Foundation for Innovation Team of Bioanalytical Chemistry.

References

1. L. Wang, J. Zhang, B. Kim, J. Peng, S. N. Berry, Y. Ni, D. Su, J. Lee, L. Yuan, and Y. Chang, *J. Am. Chem. Soc.*, 138 (2016) 10394.

2. W. Ma, D. Li, T. Sutherland, Y. Li, Y. Long, and H. Chen, *J. Am. Chem. Soc*., 133 (2011) 12366.
3. Y. Zhou, Z. Xu, and J. Yoon, *Chem. Soc. Rev*., 40 (2011) 2222.
4. Y. Kim, T. Kim, J. Ryu, and Y. Yoo, *Biosens. Bioelectron*., 25 (2010) 1160.
5. L. Li, H. Lu, and L. Deng, *Talanta*, 113 (2013) 1.
6. L. Wu, X. Zhang, and H. Ju, Anal. Chem., 79 (2007) 453.
7. J. Singh, A. Singh, and N. Singh, *RSC Adv*., 106 (2014) 61841.
8. M. Govindhan, M. Amiri, and A. Chen, *Biosens. Bioelectron*., 66 (2015) 474.
9. G. Gowda, L. Abell, C. Lee, R. Tian, and D. Raftery, *Anal. Chem.*, 88 (2016) 4817.
10. C. Chen, Y. Chen, and M. Lin, *Biosens. Bioelectron.*, 42 (2013) 379.
11. H. Li, K. Worley, and S. Barton, *ACS. Catalysis*, 12 (2012) 2572.
12. T. Canevari, R. Vinhas, R. Landers, and Y. Gushikem, *Biosens. Bioelectron*., 26 (2011) 2402.
13. C. Shan, H. Yang, D. Han, Q. Zhang, A. Ivaska, and L. Niu, *Biosens. Bioelectron.*, 25 (2010) 1504.
14. J. Goran, C. Favela, and K. Stevenson, *Anal .Chem*., 85 (2013) 9135.
15. Z. Li, Y. Huang, L. Chen, X. Qin, Z. Huang, Y. Zhou, Y. Meng, J. Li, S. Huang, Y. Liu, W. Wang, Q. Xie, and S. Yao, *Sensors and Actuators B: Chemical.*, 181 (2013) 280.
16. Y. Li, L. Shi, W. Ma, D. Li, H. Kraatz, and Y. Long, *Bioelectrochemistry*, 80 (2011) 128..
17. A. Pinczewska, M. Sosna, S. Bloodworth, J. Kilburn, and P. Bartlett, *J. Am. Chem. Soc*., 43 (2012) 18022.
18. G. Ferreira, F. Oliveira, F. Leite, C. Maroneze, L. Kubota, F. Damos, and R. Luz, *Electrochimica Acta*, 111 (2013) 543.
19. H. Li, R. Li, R. Worden, and S. Barton, *ACS. Appl. Mater. Interfaces*., 6 (2014) 6687.
20. H. Teymourian, A. Salimi, and R. Hallaj, *Biosens. Bioelectron*., 33 (2012) 60.
21. E. Sharifi, A. Salimi, and E. Shams, *Biosens. Bioelectron*., 45 (2013) 260.
22. M. Wooten, and W. Gorski, *Anal .Chem.*, 82 (2010) 1299.
23. P. Gai, C. Zhao, Y. Wang, E. Halim, J. Zhang, and J. Zhu, *Biosens. Bioelectron*., 62 (2014) 170.
24. A. Geim, *Science*, 324 (2009) 1530.
25. H. Guo, X. Wang, Q. Qian, F. Wang, and X. Xia, *ACS. Nano*., 3 (2009) 2653..
26. A. Ambrosi, C. Chua, A. Bonanni, and M. Pumera, *Chem. Rev.*, 114 (2014) 7150.
27. M. Xu, T. Liang, M. Shi, and H. Chen, *Chem. Rev*., 113 (2013) 3766.
28. Y. Li, Y. Gu, B. Zheng, L. Luo, C. Li, X. Yan, T. Zhang, N. Lu, and Z. Zhang, *Talanta*, 162 (2017) 80.
29. L. Zheng, L. Xiong, Y. Li, J. Xu, X. Kang, Z. Zou, S. Yang, and J. Xia, *Sens. Actuators B*, 177 (2013) 344.
30. M. Xu, T. Liang, M. Shi, and H. Chen, *Chem. Rev*., 113 (2013) 3766.
31. M. Liu, R. Zhang, and W. Chen, *Chem. Rev*., 114 (2014) 5117.
32. L. Guo, Q. Liu, G. Li, J. Shi, J. Liu, T. Wang, and G. Jiang, *Nanoscale*, 4 (2012) 5864.
33. D. Dreyer, D. Miller, B. Freeman, D. Paul, and C. Bielawski, *Chem. Sci.*, 4 (2013) 3796.
34. X. Shen, Y.Cui, Y. Pang, and H. Qian, *Electrochim. Acta*, 59 (2012) 91.
35. M. Tabrizi, S. Azar, and J. Varkani, *Anal. Biochem*., 460 (2014) 29.